Therapeutics, Targets, and Chemical Biology

Cancer Research

Antitumor Activity of Pyridocarbazole and Benzopyridoindole Derivatives that Inhibit Protein Kinase CK2

Renaud Prudent[1,2,3], Virginie Moucadel[1,2,3], Chi-Hung Nguyen[4], Caroline Barette[5], Frédéric Schmidt[6,7], Jean-Claude Florent[6,7], Laurence Lafanechère[5], Céline F Sautel[1,2,3], Eve Duchemin-Pelletier[1,2,3], Elodie Spreux[1,2,3], Odile Filhol[1,2,3], Jean-Baptiste Reiser[8], and Claude Cochet[1,2,3]

Abstract

The alkyloid compound ellipticine derived from the berrywood tree is a topoisomerase II poison that is used in ovarian and breast cancer treatment. In this study, we report the identification of ellipticine derivatives and their tetracyclic angular benzopyridoindole analogues as novel ATP-competitive inhibitors of the protein kinase CK2. *In vitro* and *in vivo* assays showed that these compounds have a good pharmacologic profile, causing a marked inhibition of CK2 activity associated with cell cycle arrest and apoptosis in human cancer cells. Further, *in vivo* assays demonstrate antitumor activity in a mouse xenograft model of human glioblastoma. Finally, crystal structures of CK2–inhibitor complex provide structural insights on the molecular basis of CK2 inhibition. Our work lays the foundation for development of clinically useful CK2 inhibitors derived from a well-studied scaffold with suitable pharmacokinetics parameters. *Cancer Res; 70(23); 9865–74. ©2010 AACR.*

Introduction

Protein kinases represent major therapeutic targets and several kinase inhibitors have demonstrated powerful clinical activity in pathologies in which the target kinase is dysregulated.

Protein kinase CK2 plays critical roles in cell growth, cell differentiation, apoptosis, and oncogenic transformation (1, 2). CK2 has been found dysregulated in many cancers and its dual function in promotion of cell growth and in suppression of apoptosis may be particularly relevant to its oncogenic potential (3). The recent association of aberrant CK2 expression with unfavorable prognostic markers in prostate cancer (4) and in acute myeloid leukemia (5) supports the direct implication of CK2 in tumor formation and recurrence. Indeed, CK2 is now considered as a promising therapeutic target, supporting the development of chemical inhibitors. Consequently, several classes of CK2 inhibitors have been reported showing various efficacy and specificity. Quercetin, emodin, 4,5,6,7-tetrabromo-1-benzotriazole (TBB), and indoloquinazolin derivative (IQA) are representative of main classes of ATP-competitive CK2 inhibitors (6, 7). Other families were also described, such as anthraquinone-related compounds, condensed polyphenolic, 7-substitued indoloquinazoline derivatives, and 2,8-difurandicarboxylic acid derivatives (8–11). However, so far, only a single report described a CK2 inhibitor (CX-4945; Cylene Pharmaceuticals) disclosing *in vivo* efficacy (http://www.cylenepharma.com/cylene/pr_1230934977). Thus, broadening the availability and diversity of CK2 inhibitors is warranted.

We have identified ellipticine and benzopyridoindole derivatives as new CK2 inhibitors. Ellipticine and its derivatives exhibit antitumoral properties and are established chemotherapeutics (12), acting either by distinct or common mechanisms of action. First, their intercalation in double-stranded DNA interferes with DNA replication or DNA transcription (13). Second, ellipticine induces topoisomerase II–mediated transient DNA double-strand breaks, which have been identified as the primary cellular target of the drug (14, 15). A third mechanism involves DNA adduct formation after P450 (CYP)-mediated activation of ellipticine in target tissues (16). Several studies have also reported apoptosis induction by ellipticine involving the p53 tumor suppressor protein (17–19). Finally, protein kinase inhibition may also represent a novel mechanism involved into ellipticine effect. Cdk2-dependent p53 phosphorylation is selectively inhibited by ellipticine and 9-hydroxyellipticine (20). Ellipticine derivatives have also inhibitory activity on c-Kit (21).

Here, we report that ellipticine and its benzopyridoindole derivatives are *in vitro* and *in vivo* ATP-competitive CK2

Authors' Affiliations: [1]INSERM, U873; [2]CEA, iRTSV/LTS; [3]Université Joseph Fourier, Grenoble, France; [4]UMR 176 CNRS-Institut Curie, Institut Curie Bât 110, Orsay, France; [5]CNRS, UMR 5168, CEA, iRTSV/CMBA, Grenoble, France; [6]UMR 176 CNRS-Institut Curie, Centre de Recherche; [7]CNRS, UMR 176, Paris, France; [8]Institut de Biologie Structurale Jean-Pierre Ebel, CEA-CNRS-UJF-PSB, Grenoble, France

Note: Supplementary data for this article are available at Cancer Research Online (http://cancerres.aacrjournals.org/).

Corresponding Author: Claude Cochet, INSERM, U873, CEA, iRTSV/LTS, and Université Joseph Fourier, F-38054 Grenoble, France. Phone: 33-4-38-78-42-04; Fax: 33-4-38-78-50-58; E-mail: claude.cochet@cea.fr or Jean-Baptiste Reiser, Institut de Biologie Structurale Jean-Pierre Ebel, CEACNRS-UJF-PSB, 41 rue Jules Horowitz, F-38027 Grenoble, France. Phone: 33-4-76-20-94-49; Fax: 33-4-76-20-94-80; E-mail: jean-baptiste.reiser@ibs.fr.

doi: 10.1158/0008-5472.CAN-10-0917

inhibitors displaying antitumoral activity. We provide a rationale basis for the mode of action of these compounds on the basis of the crystal structure of CK2α-inhibitor complexes. Knowing that ellipticine displays good pharmacokinetics criteria, this new class of inhibitors is a source of attractive leads for further optimization.

Material and Methods

Chemical libraries

The Institut Curie-CNRS library (6,560 compounds) and The Prestwick Chemical Library (1,120 compounds) were screened for CK2 inhibitors. Active compounds in the primary screen were retested from freshly made solutions.

Cell culture

HeLa (human cervical adenocarcinoma), U373 (human glioblastoma), MCF-10A (human mammary epithelial cells), MESSA, and MESSA Dx5 (myosarcoma) cell lines were obtained from the American Type Culture Collection (ATCC) during 2005. Cells were cultured and stored according to the supplier's instructions and used at passages 5 to 20. Briefly, cells were routinely cultivated in Dulbecco's medium (Invitrogen Life Technologies, Inc.) supplemented with 10% (v/v) fetal calf serum (BioWest), except for MCF-10A cells that were maintained in a 1:1 mixture of Dulbecco's modified Eagle's medium and Ham's F-12 medium supplemented with 5% horse serum, L-glutamine, 25 ng/mL human recombinant EGF, 100 ng/mL cholera toxin, 10 μg/mL insulin, and 0.5 μg/mL hydrocortisone. Cells were last tested in July 2009 through cell morphology monitoring, growth curve analysis, and contamination checks.

Automated screening

Automated screening of chemical libraries was performed in 96-well plates using the automated platform of the CMBA (centre de Criblage pour Molécules Bio-Actives, Grenoble) screening facilities as described in the study of Prudent et al. (22).

CK2 phosphorylation assays

Compounds were tested in a radiometric CK2 assay performed in a final volume of 18 μL containing 1 μL of compound or equivalent amount of dimethyl sulfoxide (DMSO) as control, 3 μL of CK2α (36 ng), and a mixture containing 100 μmol/L of peptide substrate (RRREDEESDDEE), 10 mmol/L $MgCl_2$, and 100 μmol/L [γ-^{32}P]-ATP (6,000 Ci/mmol). Assays were performed at room temperature for 5 minutes before termination by the addition of 60 μL of 4% trichloroacetic acid. Incorporation of ^{32}P in the peptide substrate was determined as previously described (23).

Protein purification and crystallization

A truncated active form of the catalytic α subunit of human CK2 (CK2α$^{\Delta C}$) was expressed in *Escherichia coli* and purified as described in the study of Ermakova et al. (24). CK2α$^{\Delta C}$ was first crystallized using hanging drop vapor-diffusion technique. Crystallization drops were prepared by mixing 2 μL of CK2α$^{\Delta C}$–Mg^{2+}–substrate peptide mix [4.6 mgmL-1 CK2α$^{\Delta C}$, 114 μmol/L peptide substrate RRREDEESDDEE, 680 μmol/L $MgCl_2$, 340 μmol/L adenosine 5′-(β,γ-imido)triphosphate] with 2 μL of precipitant solution (36% polyethylene glycol 5000 monomethyl ether, 150 mmol/L ammonium sulfate, and 100 mmol/L Tris-HCl, pH 7.5). Crystals of ellipticine and benzopyridoindole derivative–CK2α$^{\Delta C}$ complexes were then obtained by soaking techniques: crystals were soaked for 1 week in a 4-μL drop of same composition as crystallization drop except that adenosine 5′-(β,γ-imido)triphosphate was replaced by 300 μmol/L of these derivatives.

Structure determination and refinement

For X-ray diffraction data collection, CK2α$^{\Delta C}$ complex crystals were directly flash frozen in liquid nitrogen without adding any extra cryoprotectant. All data were collected at −173.15°C on beamlines of either ID23-eh1 or ID23-eh2 of the European Synchrotron Radiation Facility (ESRF) at a wavelength of 1.072 or 0.834 Å using an ADSC Quantum 315R CCD detector. Data processing was performed using XDS (25) and summarized in Supplementary Table S1. The CK2α$^{\Delta C}$ complex structures were determined by molecular replacement method with AMoRe (26) from the CCP4 suite (27) using the CK2α$^{\Delta C}$ structure as search model [pdb code: 1PJK, (24)]. The final models were obtained after several rounds of alternate manual building with coot (28) and maximum likelihood refinement with Refmac5 of CCP4 (29), and using data in all available resolution range. The final refinement statistics are summarized in Supplementary Table S1. Pymol was used to generate structure figures. The structure factors and coordinates are deposited in the Protein Data Bank (PDB) under the accession numbers: 3OWJ, 3OWK, and 3OWL.

Kinase selectivity profiling

Kinase selectivity of compound **18** was assessed using a panel of 57 recombinant protein kinases. The assays were performed at 10 μmol/L ATP in the presence of 10 μmol/L inhibitor using the Kinase profiler panel service (Millipore). Inhibition, expressed as the percent of activity determined in the absence of inhibitor, was calculated from the residual activity measured in the presence of 10 μmol/L inhibitor.

Cellular CK2 activity assay

Cellular CK2 activity was assayed as previously described (22, 30). Briefly, HeLa cells were transfected with a chimeric yellow fluorescent protein–based CK2 activity reporter (pEYFPc1-SβS). Phosphorylation status of the reporter was measured using the monoclonal antibody anti-GFP/yellow fluorescent protein (Roche, ref. 1814460) at 1/1,000 and the goat anti-mouse HRP as secondary antibody (Sigma, ref. A4416).

Murine xenograft tumor assay

All experimental procedures adhered to our local ethical committee (Comité régional d'éthique pour l'Expérimentation animale CREEA, Rhône Alpes, protocol no. 286). Female Harlan athymic nude mice (6–8 weeks) were inoculated subcutaneously into the right flank with 7.5×10^5 U373 cells. When tumors reached ±50 mm^3 (volume = length × width × height), animals were treated intraperitoneally

3 times weekly (every 2 days) for 2 weeks, with compound **19** (0.14 mg/100 μL per injection), or equivalent amount of DMSO (10% final) dissolved in PEG3350 22.5%, bovine serum albumin 0.45%. Body weight and tumor volume were determined twice a week. The experiment was terminated when tumor volume reached about 1,000 mm^3. Results are presented as mean ± SEM.

Results

Discovery of new CK2 inhibitors by automated screening

So far, only few CK2 inhibitors display suitable pharmacokinetics criteria for *in vivo* investigations. To find new CK2 inhibitor scaffolds appropriate for *in vivo* uses, we screened the Prestwick Chemical Library. This library contains small molecules that were selected for their known bioavailability and safety in humans. The expectation was to identify hits that exhibit correct bioavailability and toxicity. These hits could provide good starting points for optimization program.

The library was screened in an automated luminescence-based kinase assay using human recombinant CK2α catalytic subunit (Supplementary Fig. S1). Screening data were normalized and analyzed using an in-house software, TAMIS (Tool to Analysis and Manage Informations of Screening, Version 2.0; CEA, Grenoble, France). CK2 kinase inhibitory activity was determined at compound concentration of 10 μmol/L, using TBB and DMSO as positive and negative controls, respectively.

Up to 24 compounds belonging to several distinct structural families showed inhibition greater than 50%. Among those hits, ellipticine was the only drug with therapeutic indication in oncology. To identify more potent and selective CK2 inhibitors we performed a focused screen on ellipticine derivatives present in the Institut Curie-CNRS small molecule library (Supplementary Fig. S1).

This led to the identification of benzopyridoindole derivatives (31, 32). Radiometric CK2 kinase assay showed that 1, 8, 16, 18, 19 efficiently inhibited kinase activity in a dose-dependent manner (Table 1) with IC_{50} ranging from 0.31 to 1.5 μmol/L. This represents a 10- to 50-fold improvement in inhibitor potency when compared with our primary hit, ellipticine (in these conditions, IC_{50} for ellipticine is 15.4 μmol/L).

Chemical features of pyridocarbazole derivatives conferring CK2 inhibitory potency

To define the mode of CK2 inhibition by compound **1**, we performed steady-state kinetic analysis (Supplementary Fig. S2). Lineweaver–Burk inhibition plots showed that CK2 inhibition by compound **1** is ATP competitive, with K_i = 0.86 μmol/L . Similar inhibitory potencies were found using CK2 holoenzyme (data not shown).

To gain insights into the features conferring inhibitory potency to compound **1**, we tested a set of derivatives (Table 1). Position 11 is relatively tolerant because substitution of methyl by hydrogen also leads to an active compound (compound **8**) albeit less potent. In contrast, the free hydroxyl substituent at position 9 (compounds **1** and **8**) is necessary because analogues bearing substituents other than hydroxyl (e.g., ether, ester) are less active or inactive even when assayed at 10 μmol/L (compounds **2**, **4**, **6**, **7**, **9**, **10**, **11**, **12**, **13**, **14**, **15**, and **17**).

Similarly, methylation of N2 is also not tolerated because compound **3** is inactive. In line with this observation, compound **5**, which is fully substituted at positions 2, 9, and 11, is also inactive. Position 1 also seems to be relatively tolerant because replacement of lactam function (compound **8**) by chloro group (compound **16**) leads to active compound. Whether compounds **11**, **12**, and **13** are inactive because position 9 bears methoxy group or position 1 bears too bulky/hydrophobic substituents remains unknown.

Interestingly, although compounds **14**, **15**, and **17** bear methoxy groups at position 9, they display residual inhibitory potency. In the same trend, ellipticine is active (albeit at higher concentration). This observation indicates that unfavorable substitution at this important position can be counterbalanced by a network of favorable substitutions at other positions. We next investigated the features of the scaffold required for activity. Available pyridoindole (or γ-carboline) derivatives bearing 3 fused rings exhibit poor or no activity (data not shown), meaning that 4 rings are necessary for optimal activity. We tested several available angular tetracyclic compounds related to intoplicine, which corresponds to antitumor agent inhibiting both topoisomerase I and II activities (33). Surprisingly, 2 compounds belonging to benzo[*g*]- and benzo[*e*]-pyridoindole (or BgPI and BePI) (compounds **18** and **19**, respectively) are potent CK2 inhibitors (Table 2). This indicates some tolerance into the scaffold of these new CK2 inhibitors.

In summary, regarding linear tetracyclic ellipticine derivatives, it appears that positions 9 and N2 are crucial for activity whereas positions 1 and 11 are relatively tolerant. Moreover, some variations into the scaffold of the molecule are allowed. Indeed, the angular tetracyclic analogues BgPI and BePI, which are structurally related to ellipticine, also exhibit significant CK2 inhibitory potencies.

Pyridocarbazole derivatives are multitarget compounds

Given the multiple targets of ellipticine and derivatives, we compared our structure-activity relationship data with published data (Supplementary Table S2), and on c-Kit (21) and topoisomerase II (15). This analysis showed differences in structure-activity relationship according to the targets. For instance, whereas C1 substitution does not have a strong influence on topoisomerase II and CK2α activities, it is detrimental on c-Kit inhibitory potency when substituted by bulky groups. In contrast, N2 substitution is detrimental for CK2α inhibitory potency, but has no effect on topoisomerase II and c-Kit inhibition. N6 substitution has no influence on topoisomerase II, but is detrimental for c-Kit and CK2α inhibition. A common feature of the 3 targets is the presence of hydroxyl on position 9 in active compounds. Taken together, these observations indicate that distinct chemical requirements are necessary to selectively inhibit each of the 3 targets.

Table 1. Biochemical characterization of pyridocarbazole and B[g/e]PI in aminophenyl-4-methanesulfonamide

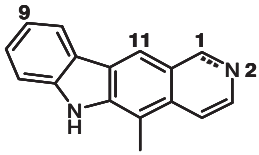

1-17

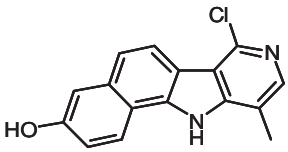

18

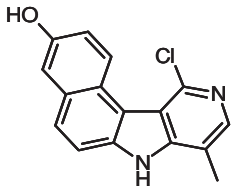

19

Compound	1-2 Bond	Substituents at position 1	2	9	11	CK2 residual activity	c-Kit residual activity	Topoisomerase IIα residual activity	DNA intercalation
1	Single	C=O	H	OH	Me	4.5	79.9	97.8	65.1
2	Single	C=O	H	OMe	Me	99.5	131.2	94.2	52.0
3	Single	C=O	Me	OH	H	99.0	96.5	100.0	72.9
4	Single	C=O	H	OMe	H	100.1	81.4	99.2	66.8
5	Single	C=O	Bz	OBz	Me	100.1	183.3	133.6	71.2
6	Single	C=O	H	OBz	Me	100.1	103.5	112.2	46.9
7	Single	C=O	H	OAc	H	100.1	110.3	88.3	81.3
8	Single	C=O	H	OH	H	9.7 (IC_{50}=1.5 μmol/L)	88.8	65.3	79.4
9	Single	C=O	H	OBn	H	99.0	110.5	69.7	93.4
10	Single	C=O	H	OBn	Me	99.9	95.2	39.2	52.2
11	Double	A	H	OMe	Me	100.0	88.5	73.7	52.9
12	Double	B	H	OMe	H	99.8	90.9	37.3	69.4
13	Double	HNPh	Me	OMe	H	100.1	142.7	81.5	88.3
14	Double	CN	/	OMe	H	62 (IC_{50} > 15 μmol/L)	65.7	103.4	58.9
15	Double	Cl	/	OMe	Me	56.7 (IC_{50} > 15 μmol/L)	93.3	74.5	65.5
16	Double	Cl	/	OH	H	4 (IC_{50} = 1.4 μmol/L)	70.3	115.0	68.7
17	Double	H	Tosyl	OMe	Me	52.3 (IC_{50} > 15 μmol/L)	61.4	82.8	91.7
18						1.4 (IC_{50} = 1.5 μmol/L)	60.4	106.8	62.0
19						3.5 (IC_{50} = 0.67 μmol/L)	16.9	77.0	66.4

CK2α and c-Kit kinase assays and topoisomerase IIα assay were performed at 10 μmol/L compound concentration. DNA intercalation assay was performed at 2.5 μmol/L compound concentration.

Table 2. Biochemical characterization of pyridocarbazole and B[g/e]PI in Aminophenyl-2-methoxy-4-methanesulfonamide

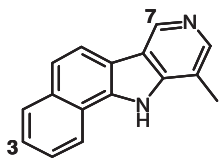

18-20-21

Compound	7-8 Bond	Substituents at position 3	7	CK2 residual activity
18	Double	OH	Cl	1.4 (IC_{50} = 1.5 μmol/L)
20	Double	OMe	Cl	94.0
21	Single	OMe	C=O	80.0

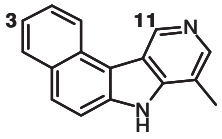

19-22-23

Compound	10-11 Bond	Substituents at position 3	11	CK2 residual activity
19	Double	OH	Cl	3.5 (IC_{50} = 0.67 μmol/L)
22	Double	OMe	Cl	73.0
23	Single	OMe	C=O	82.0

CK2α assays were performed at 10 μmol/L compound concentration. All results are expressed as percentage of activity without inhibitor.

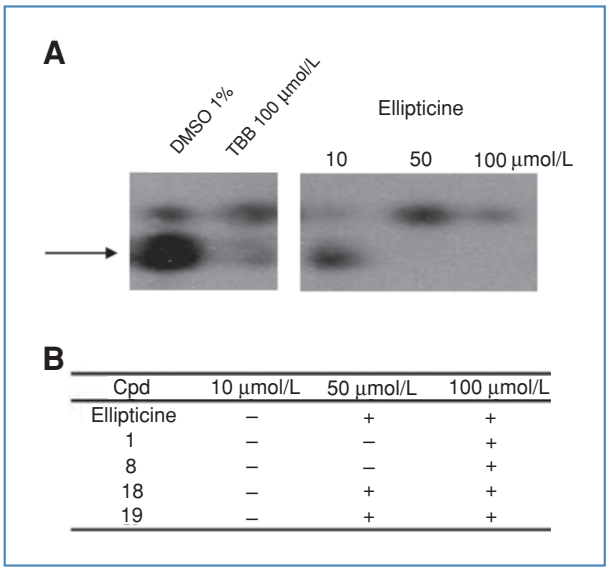

Cpd	10 μmol/L	50 μmol/L	100 μmol/L
Ellipticine	–	+	+
1	–	–	+
8	–	–	+
18	–	+	+
19	–	+	+

Figure 1. A, ellipticine inhibition of CK2 activity in living cells. HeLa cells transfected with a plasmid expressing a chimeric CK2 activity GFP-based reporter were incubated with the CK2 inhibitor TBB, ellipticine, or DMSO (as control) for 24 hours. Cell extracts were then analyzed by native electrophoresis and GFP was revealed by immunoblotting. The arrow indicates the CK2-phosphorylated form of the reporter. B, selected derivatives that were active *in vitro* were submitted to the cell-based CK2 activity assay as in A. +, a significant decrease in the phosphorylated form of the CK2 activity reporter (lower band in A and in Supplementary Fig. S3).

Pyridocarbazole derivatives are cell-potent CK2 inhibitors

We assayed the inhibitory potencies of pyridocarbazole derivatives on living cells using a cell-based CK2 kinase assay (Fig. 1) (22, 34). In control HeLa cells, the CK2 activity reporter could be detected as a phosphorylated form (lower band in Fig. 1A). When cells were treated with the known CK2 inhibitor TBB, the phosphorylated CK2 reporter form disappeared. Interestingly, 50 μmol/L ellipticine triggered a similar strong inhibition (Fig. 1A). Other derivatives selected in the present work were found to be active in cells at similar or even lower concentrations (compounds **1**, **8**, **18**, **19**) (Fig. 1B; Supplementary Fig. S3).

Ellipticine and B[g/e]PI derivatives inhibit cell viability through cell cycle arrest and apoptosis

Because both ellipticine and CK2 inhibitors are known to affect cell survival, we measured cell viability of $p53^{wt}$ HeLa cells after 48-hour treatment with TBB, ellipticine, or angular compounds **18** and **19** (Fig. 2A). B[g/e]PI derivatives reduced cell viability more efficiently than TBB (IC_{50} of 2–10 μmol/L and 20 μmol/L, respectively). Interestingly, in $p53^{mut}$ U373 glioblastoma cells, 5 μmol/L of pyridocarbazole derivatives was sufficient to decrease cell viability by 50% whereas in these conditions, TBB was not efficient (Fig. 2B). U373 cells harbor a TP53 mutant isoform and are particularly resistant to drug-induced apoptosis. Other cancer cell lines such as wild-type or resistant myosarcoma cells (MESSA and MESSA Dx5, respectively) were highly sensitive to ellipticine and to a lower extent to compounds **18** and **19.** Of note, the cell viability of the nontransformed MCF10A mammary epithelial cells was also strongly affected by ellipticine, whereas compounds **18** and **19** had a much weaker effect. As cell viability inhibition induced by ellipticine was reported to be correlated with cell cycle arrest (35), we measured the effect of ellipticine and B[g/e]PI derivatives on cell cycle distribution of HeLa and U373 cells (Fig. 3A). Compared with vehicle-treated cells, **18**- or **19**-treated U373 cells exhibited a cell cycle arrest in G_2/M phase. The treatment also caused an appreciable accumulation of the cells in sub-G_1 phase. We next assessed the effects of the compounds on the induction of apoptosis in U373 cells by (terminal deoxynucleotidyl transferase-mediated dUTP nick end labeling (TUNEL). The results showed that 18 or 19 treatment results in the accumulation of TUNEL-positive cells. This effect was more pronounced with Ellipticine or staurosporine treatments (Fig. 3B). Moreover, the same treatments induced an increase of caspase-dependent apoptosis attested by the activation of caspase 3/7 activity (Fig. 3C).

Although these compounds are cell-potent CK2 inhibitors, we noticed that except for ellipticine, the active concentrations able to induce marked CK2 inhibition were higher than those required to induce cytotoxicity. Ellipticine is known as a multitarget agent, thus our selected active benzopyridoindole derivatives could, beside CK2α, affect other targets involved in cell viability. Indeed, when kinase selectivity of compound **18** was profiled, several kinases involved in cancer-related pathways such as Pim-1, Mnk2, and DARK1 were significantly affected (Supplementary Table S3).

Benzopyridoindole derivatives inhibit colony formation and tumor growth

To ascertain the potential therapeutic interest of compounds **18** and **19**, we first tested their ability to inhibit colony formation using soft agar assay as an *in vitro* surrogate of tumorigenesis. U373 cells can grow without anchorage and form colonies in soft agar culture, reflecting their malignant properties. Both compounds **18** and **19** at a concentration of 5 μmol/L inhibited drastically colony formation (Fig. 4A). In comparison, a weak inhibition of colony formation (10%) was observed in response to 50 μmol/L of TBB (data not shown).

Next, murine xenograft tumor assays were carried out to assess both toxicity and efficiency of compound **18**, which showed the best inhibitory activities toward cell viability and colony formation. In mice treated with compound **18,** we observed a significant reduction of tumor incidence, whatever the time point. Three weeks after first compound injection, mice injected with compound **18** had tumors that were 5 to 6 times smaller than those injected with DMSO (Fig. 4B). Furthermore, mice were healthy after repetitive injections of the compound. They grew normally without significant weight loss. In addition, no obvious toxic effects were observed when the experiment was terminated and the tumors removed, indicating that compound **18** was relatively well tolerated at doses sufficient to induce antitumoral effect.

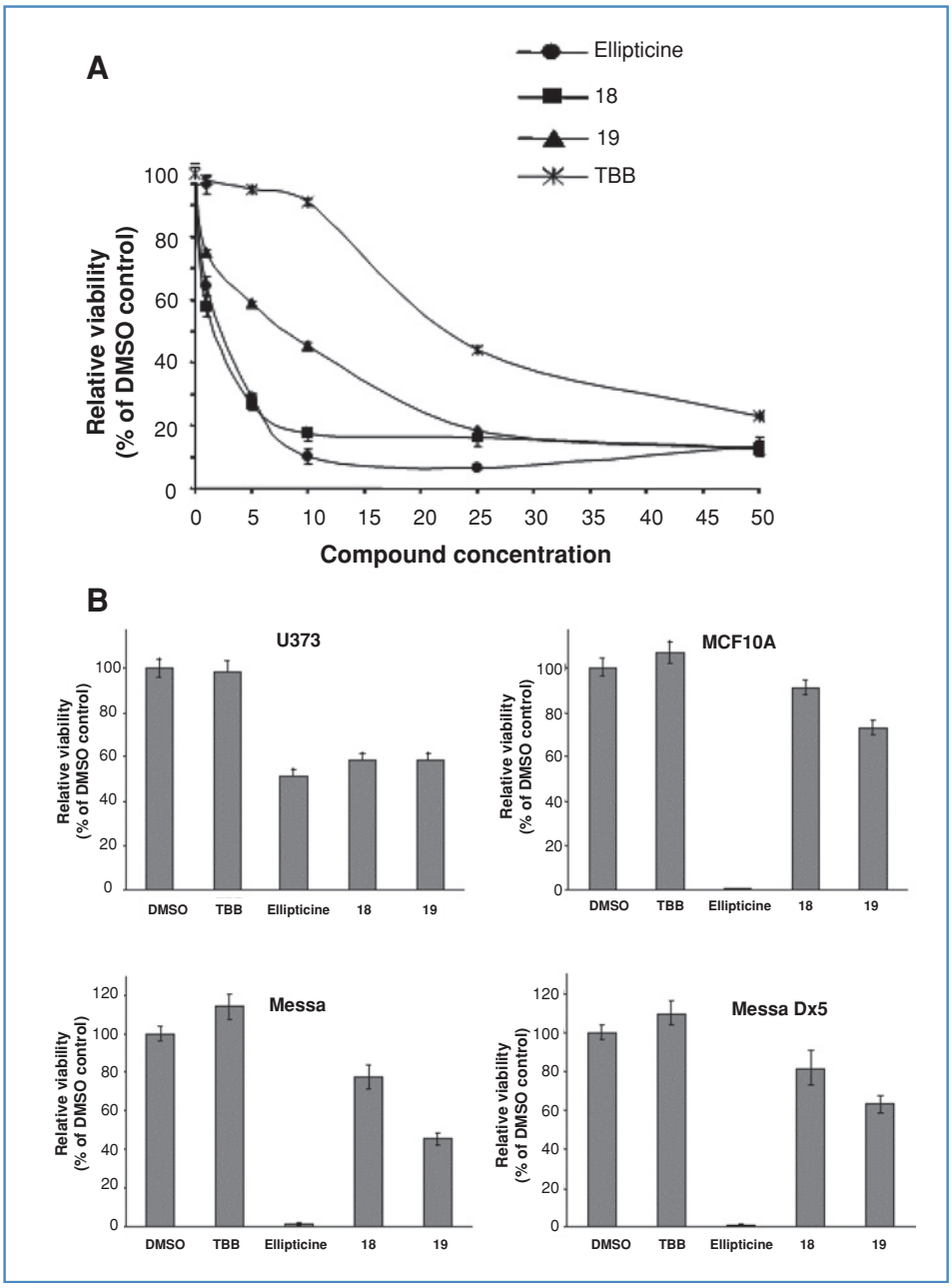

Figure 2. Effect of ellipticine and B[g/e]PI derivatives on cell viability. A, HeLa cells were incubated with increasing amount of compounds for 48 hours and cell viability was assayed by the Cell Titer Glo Luminescent Cell Viability Assay (Promega). Results are given relative to the luminescence recorded for DMSO. Experiment was done in triplicate and repeated twice. B, different cell lines as indicated were incubated with 5 μmol/L compounds or equivalent amount of DMSO as control. Two days later, living cells were counted as in A. Results are given relative to the luminescence recorded for DMSO. Data are representative of 2 experiments performed in triplicate.

X-ray crystallographic structures of CK2–inhibitor complexes

To gain insights at the atomic level into the mode of action of these new inhibitors, we solved the structure of the truncated active form of CK2α in complex with pyridocarbazole and B[g/e]PI derivatives by X-ray crystallography: compound **1**/CK2α at 1.85 Å resolution, compound **18**/CK2α at 1.80 Å resolution, and compound **19**/CK2α at 2.1 Å resolution (Fig. 5). Electron densities of compounds **1**, **18**, and **19** are well defined and lead to no ambiguity regarding their orientations and positions in the ATP binding site. Commonly, the interaction between the 3 compounds and CK2 are mainly hydrophobic and involve mainly residues 53, 66, and 174. They use the plane formed by 2 adjacent cycles to fit perfectly into the "purine plane" naturally occupied by the ATP adenine moiety (24, 36). However, they differ in their orientation to conserve specific interactions between the common atoms of their scaffold and of the ATP groove. For instance, the common hydroxyl group (at position 9) of the 3 derivatives forms a direct hydrogen bond with the main chain nitrogen of Val 116 that mimics the classical ATP/CK2 interaction. But, the

A

U373	DMSO	Ellipticine	18	19
Sub-G1	3.26 ± 0.11	8.75 ± 0.37	10.26 ± 0.36	11.59 ± 0.56
G1	62.33 ± 1.28	36.11 ± 0.21	53.84 ± 0.23	48.19 ± 0.48
S	15.82 ± 0.60	23.37 ± 2.44	8.09 ± 0.10	12.62 ± 0.91
G2/M	19.02 ± 0.84	32.93 ± 1.22	28.04 ± 0.07	27.70 ± 0.11

HeLa	DMSO	Ellipticine	18	19
Sub-G1	0.73 ± 0.06	1.02 ± 0.21	0.74 ± 0.07	1.29 ± 0.3
G1	56.14 ± 0.04	27.06 ± 0.03	47.42 ± 0.41	43.15 ± 0.17
S	4.10 ± 0.11	13.21 ± 1.76	5.94 ± 0.09	13.22 ± 0.29
G2/M	38.42 ± 0.2	57.44 ± 0.19	44.76 ± 0.28	40.04 ± 0.36

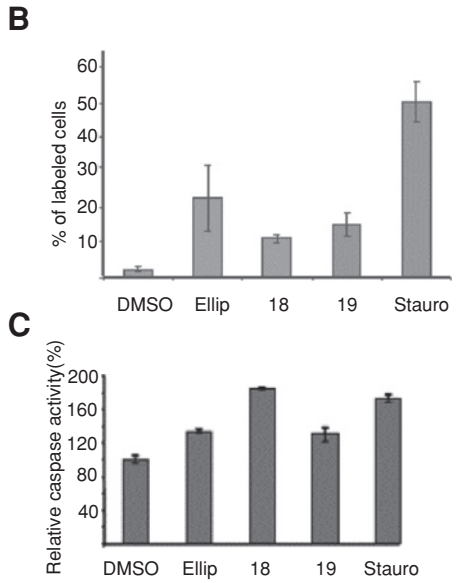

Figure 3. Ellipticine and B[g/e]PI derivatives promote cell cycle arrest and apoptosis. A, nearly confluent HeLa or U373 cells were treated with 5 μmol/L compounds or equivalent amount of DMSO. After 24 hours, cells were harvested and labeled with propidium iodide. DNA content was analyzed with FACScalibur and Cell Quest software. Percentage of HeLa or U373 cells in sub-G_1, G_1, S, and G_2/M phases are summarized. Experiment was repeated twice. B, U373 cells were treated with 5 μmol/L ellipticine (Ellip) and compounds **18** and **19** for 48 hours or with staurosporine (Stauro) for 4 hours. Then, TUNEL staining was measured with the DNA Fragmentation Kit (Calbiochem) according to the manufacturer recommendations. Around 200 cells were counted in randomly selected fields, for each point. C, U373 cells were treated with 5 μmol/L compounds for 24 hours. Then, caspase 3/7 activation was measured with the Caspase-Glo 3/7 Assay (Promega) according to the manufacturer recommendations. Data are representative of 2 experiments performed in triplicate.

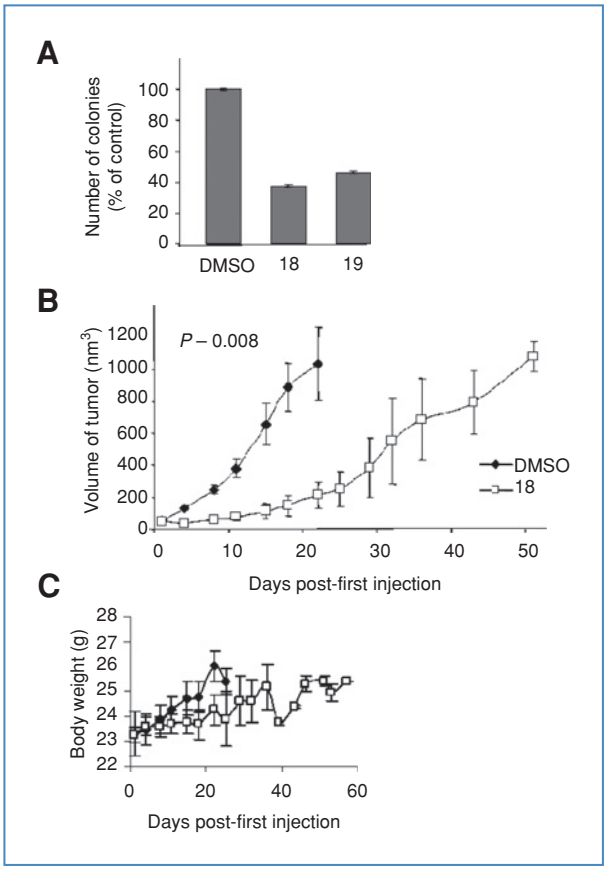

Figure 4. Compound **18** reduces colony formation *in vitro* and tumor growth *in vivo*. A, soft agar assay for colony formation. Experiment was done in duplicate at least 3 times. B, murine xenograft tumor growth assay. Athymic nude mice were inoculated subcutaneously into the right flank with 7.5×10^5 U373 cells. When tumors reached 50 mm^3, mice were injected intraperitoneally every 2 days for 2 weeks with compound **18** or equivalent amount of DMSO. Body weight and tumor volume were determined 2 times weekly. Results are presented as mean ± SEM.

differences in geometry and orientation lead them to interact differently with the bottom of the binding pocket. Compound **1** fits into the ribose pocket and partially the α-phosphate site and interacts with the catalytic site via water molecules that connect N6 of compound **1** to the main chain of Asp 174 and the catalytic dyad (Lys68/Glu81). In addition, compound **1** is further stabilized by the external side of the ATP pocket by the mean of a π-interaction between its cycle D and the Histidine at position 160 (Supplementary Table S2). By contrast, compounds **18** and **19** are rotated by 180-degree rotation and binds deeply into the α-phosphate site to directly make a hydrogen bond between their nitrogen atom of chloropyridine group and Lys68 Nz atom.

Discussion

Despite many published CK2 inhibitors with various modes of inhibition (37, 38), only few were successfully validated *in vivo*. In this work, first we report that pyridocarbazole and its angular analogues B[g/e]PI are *in vitro* potent submicromolar ATP-competitive CK2α inhibitors. Substitution requirements in pyridocarbazole derivatives are different for efficient inhibition of CK2 than substitution required for other known ellipticine targets (c-kit, topoisomerase IIα, DNA intercalation). This can give guidelines for compound optimization. Second, these compounds are also active on cellular CK2 kinase activity and induce cell cycle arrest of a glioblastoma cell line.

Proteins involved in the cells' suicide program such as ARC, Bid, and p53 (2) are some of the many cellular substrates of

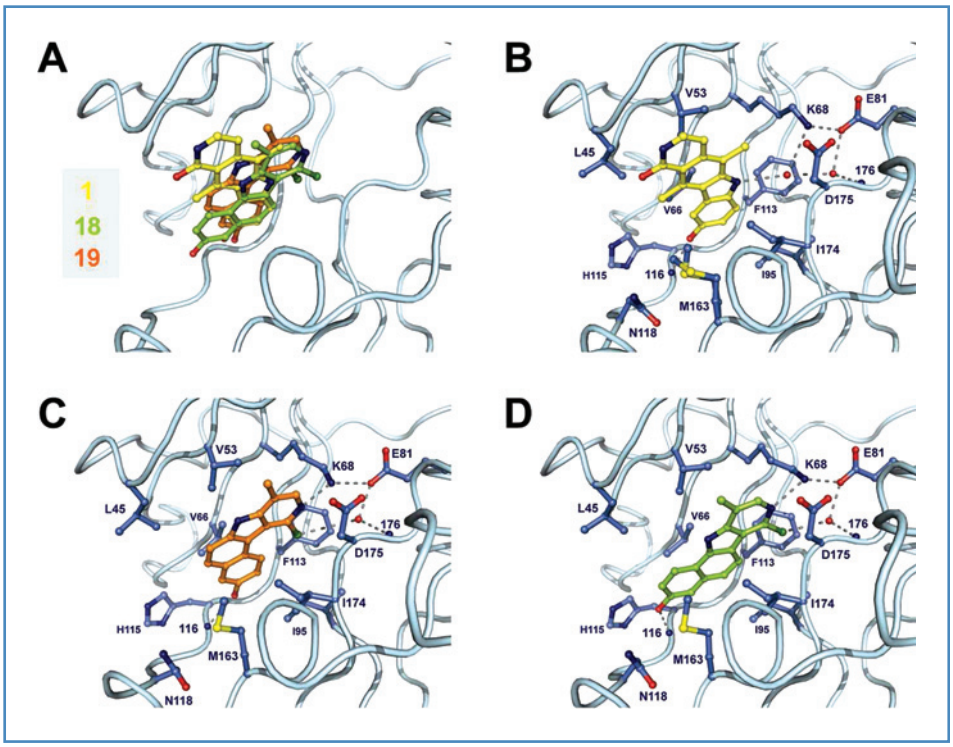

Figure 5. Close view of the structure of ellipticine and angular analogue derivatives in complex with CK2. A, superimposition of 3 CK2α–inhibitor complexes. B, CK2α–compound **1** complex structure. C, CK2α–compound **19** complex structure. D, CK2α–compound **18** complex structure. For all panels, CK2α is represented in light blue coils and CK2α residues involved in direct interaction with the compounds in darker blue ball-and-sticks. Hydrogen bonds between CK2α atoms and these derivatives are highlighted in gray dashed lines. Compounds are represented in ball and sticks: **1** in yellow, **18** in green, and **19** in orange. Atoms are colored according to their nature: red, O; blue, N; light yellow, S; dark green, Cl.

CK2 (39). Indeed, we observed that in response to pyridocarbazole derivatives, HeLa cells showed caspase-dependent apoptosis. Cytotoxic effect may be partially due to CK2 inhibition because cytotoxicity appeared at concentrations lower than those required to achieve complete CK2α inhibition. Most of cancer cells rely, however, on high CK2 activity as judged from their susceptibility to CK2 inhibitors or silencing of CK2 catalytic subunits (40). This undue reliance of tumor cells on CK2 activity may explain their high sensitivity to the pyridocarbazole derivatives. Another explanation is that these compounds target other cellular proteins such as prosurvival kinases. Indeed, kinase selectivity profiling of compound **18** showed that several kinases were significantly affected: Pim-1 and Mnk2, which are involved in cancer-related pathways (41), and DRAK1, which is related to death-associated protein kinases that trigger apoptosis (42). It is now accepted that high specificity is not a requisite for potent drugs (43) and that polypharmacology is an underlying mechanism essential in drug actions (43). Indeed, hitting more than 1 kinase at once can prevent cells to bypass the primary target by activating redundant signaling pathways (44). Interestingly, when assayed in a murine xenograft tumor growth assay, 1 of our compounds (**18**) exhibited antitumoral activity without apparent toxic effects. We conclude that this chemical class of leads seems to be safe enough to represent a good starting point for future optimization.

We have solved 3 CK2α–inhibitor complex structures. Crystal structure of CK2–compound **1** complex provides a clear explanation for the differential potency of various pyridocarbazole derivatives. The intolerance to any substitution except hydroxyl group at position 9 is fully explained by the crucial hydrogen bond that compound **1** makes with CK2α backbone, and that mimics interactions between ATP and CK2. However, the disruption of this crucial hydrogen bond can be partially compensated by extra interactions involving other residues as in compounds **14**, **15**, and **17**, which bear polar groups either at position 1 or at position 2 and have residual inhibition capacity. Those groups would be there in favorable position to interact with CK2α residues Leu45 and His160. This is exemplified by the substitution in compound **16** , which bears a chlorine group as compound **15** and a hydroxyl group as compound **1**, and retains full inhibition potency. However, in contrast to CK2α–compound **1** structure, the structures of CK2α in complex with compounds **18** and **19** revealed that their orientations are flipped by 180 degree, which lead their chlorine group to fit into the ATP cavity. Therefore, the position of such polar group cannot easily be predicted. Concerning position 11, reduction of this group volume by the substitution of a methyl group (in compound **1**) by an atom of hydrogen (in compound **3**) is correlated with a decreased inhibition (higher IC_{50}). This can be easily explained by the disruption of hydrophobic contacts between the methyl group and Met163 and Leu45 of CK2α. However, as the number of those contacts is in minority as compared with the overall network between compound **1** and CK2α, this disruption has a limited impact on IC_{50} suggesting that position 11 would be tolerant to bulkier substituents. The structures of CK2α in complex with compounds **18** and **19** illustrate the ability of the CK2 ATP-binding groove to bind benzopyridoindole derivatives with "cycle" configurations different from the original ellipticine, as long as they remain perfectly plane to fit into the purine plane. Furthermore, it appears crucial to keep the OH group at position 9 to mimic ATP/CK2 interaction as for compound **1**.

To conclude, this class of pyridocarbazole and benzopyridoindole derivatives has a well-mastered chemistry and displays new biological activities and good pharmacokinetic profile. Its high potency, the well-explored structure-activity relationship and the solved structure of these compounds in complex with CK2 will provide a good starting point for further optimization processes.

Disclosure of Potential Conflicts of Interest

No potential conflicts of interest were declared.

Acknowledgments

The authors thank the ChemAxon company (http://www.chemaxon.com), which has allowed the academic TAMIS software team (especially C. Charavay and S. Roy) to freely use the MarvinView package, a helpful Graphic User Interface for viewing structure files and query results. The authors also thank Drs. Marie-Paule Teulade-Fichou and David Monchaud for providing reagents and protocol for DNA intercalation assays. We thank H. Pointu and technicians for their efficiency for animals care. Special thanks to Juan-Carlos Fontecilla-Camps for the use of his lab facilities for crystallization, and MX group and local contacts of ESRF for their help in data collection on beamlines.

Grant Support

This work was supported by the Institut National de la Santé et de la Recherche Médicale (INSERM), the Centre National pour la Recherche Scientifique (CNRS), the Commissariat à l'Energie atomique (CEA), the Institut Curie, the Ligue Nationale Contre le Cancer (équipe labellisée 2003–2012), the Institut National du Cancer (grant number 57). R. Prudent received a fellowship for the Fondation pour la Recherche Médicale.

Received 03/17/2010; revised 09/28/2010; accepted 09/30/2010; published OnlineFirst 11/30/2010.

References

1. Ahmed K, Gerber DA, Cochet C. Joining the cell survival squad: an emerging role for protein kinase CK2. Trends Cell Biol 2002;12:226–30.
2. Litchfield DW. Protein kinase CK2: structure, regulation and role in cellular decisions of life and death. Biochem J 2003;369:1–15.
3. Tawfic S, Yu S, Wang H, Faust R, Davis A, Ahmed K. Protein kinase CK2 signal in neoplasia. Histol Histopathol 2001;16:573–82.
4. Laramas M, Pasquier D, Filhol O, Ringeisen F, Descotes JL, Cochet C. Nuclear localization of protein kinase CK2 catalytic subunit (CK2alpha) is associated with poor prognostic factors in human prostate cancer. Eur J Cancer 2007;43:928–34.
5. Kim JS, Eom JI, Cheong JW, Choi AJ, Lee JK, Yang WI, et al. Protein kinase CK2alpha as an unfavorable prognostic marker and novel therapeutic target in acute myeloid leukemia. Clin Cancer Res 2007;13:1019–28.
6. Pagano MA, Cesaro L, Meggio F, Pinna LA. Protein kinase CK2: a newcomer in the 'druggable kinome'. Biochem Soc Trans 2006;34:1303–6.
7. Duncan JS, Gyenis L, Lenehan J, Bretner M, Graves LM, Haystead TA, et al. An unbiased evaluation of CK2 inhibitors by chemo-proteomics: characterization of inhibitor effects on CK2 and identification of novel inhibitor targets. Mol Cell Proteom 2008;7:1077–88.
8. De Moliner E BN, Johnson LN. Alternative binding modes of an inhibitor to two different kinases. Eur J Biochem 2003;270:3174–81.
9. Meggio F, Pagano MA, Moro S, Zagotto G, Ruzzene M, Sarno S, et al. Inhibition of protein kinase CK2 by condensed polyphenolic derivatives. An *in vitro* and *in vivo* study. Biochemistry 2004;43:12931–6.
10. Loizou JI, El-Khamisy SF, Zlatanou A, Moore DJ, Chan DW, Qin J, et al. The protein kinase CK2 facilitates repair of chromosomal DNA single-strand breaks. Cell 2004;117:17–28.
11. Lopez-Ramos M, Prudent R, Moucadel V, Sautel CF, Barette C, Lafanechère L, et al. New potent dual inhibitors of CK2 and Pim kinases: discovery and structural insights. FASEB J. 2010;24:3171–85.
12. Auclair C. Multimodal action of antitumor agents on DNA: the ellipticine series. Arch Biochem Biophys 1987;259:1–14.
13. Kohn KW, Waring MJ, Glaubiger D, Friedman CA. Intercalative binding of ellipticine to DNA. Cancer Res 1975;35:71–6.
14. Tewey KM, Chen GL, Nelson EM, Liu LF. Intercalative antitumor drugs interfere with the breakage-reunion reaction of mammalian DNA topoisomerase II. J Biol Chem 1984;259:9182–7.
15. Fosse P, Rene B, Le Bret M, Paoletti C, Saucier JM. Sequence requirements for mammalian topoisomerase II mediated DNA cleavage stimulated by an ellipticine derivative. Nucleic Acids Res 1991;19:2861–8.
16. Stiborova M, Breuer A, Aimova D, Stiborova-Rupertova M, Wiessler M, Frei E. DNA adduct formation by the anticancer drug ellipticine in rats determined by 32P postlabeling. Int J Cancer 2003;107:885–90.
17. Peng Y, Li C, Chen L, Sebti S, Chen J. Rescue of mutant p53 transcription function by ellipticine. Oncogene 2003;22:4478–87.
18. Sugikawa E, Hosoi T, Yazaki N, Gamanuma M, Nakanishi N, Ohashi M. Mutant p53 mediated induction of cell cycle arrest and apoptosis at G1 phase by 9-hydroxyellipticine. Anticancer Res 1999;19:3099–108.
19. Kuo YC, Kuo PL, Hsu YL, Cho CY, Lin CC. Ellipticine induces apoptosis through p53-dependent pathway in human hepatocellular carcinoma HepG2 cells. Life Sci 2006;78:2550–7.
20. Ohashi M, Sugikawa E, Nakanishi N. Inhibition of p53 protein phosphorylation by 9-hydroxyellipticine: a possible anticancer mechanism. Jpn J Cancer Res 1995;86:819–27.
21. Vendome J, Letard S, Martin F, Svinarchuk F, Dubreuil P, Auclair C, et al. Molecular modeling of wild-type and D816V c-Kit inhibition based on ATP-competitive binding of ellipticine derivatives to tyrosine kinases. J Med Chem 2005;48:6194–201.
22. Prudent R, Moucadel V, Lopez-Ramos M, Aci S, Laudet B, Mouawad L, et al. Expanding the chemical diversity of CK2 inhibitors. Mol Cell Biochem 2008;316:71–85.
23. Filhol O, Cochet C, Delagoutte T, Chambaz EM. Polyamine binding activity of casein kinase II. Biochem Biophys Res Commun 1991;180:945–52.
24. Ermakova I, Boldyreff B, Issinger OG, Niefind K. Crystal structure of a C-terminal deletion mutant of human protein kinase CK2 catalytic subunit. J Mol Biol 2003;330:925–34.
25. Kabsch W. Automatic processing of rotation diffraction data from crystals of initially unknown symmetry and cell constants. J Appl Cryst 1993;26:795–800.
26. Navaza J. AMoRe: an automated package for molecular replacement. Acta Cryst 1994;A50:157–63.
27. Collaborative Computational Project, Number 4. The CCP4 suite: programs for protein crystallography. Acta Crystallogr D Biol Crystallogr 1994;50:760–3.
28. Emsley P, Cowtan K. Coot: model-building tools for molecular graphics. Acta Crystallogr D Biol Crystallogr 2004;60:2126–32.
29. Murshudov GN, Vagin AA, Dodson EJ. Refinement of macromolecular structures by the maximum-likelihood method. Acta Crystallogr D Biol Crystallogr 1997;53:240–55.
30. Prudent R, Lopez-Ramos M, Moucadel V, Barette C, Grierson D, Mouawad L, et al. Salicylaldehyde derivatives as new protein kinase CK2 inhibitors. Biochim Biophys Acta 2008;1780:1412–20.
31. Nguyen CH, Lhoste JM, Lavelle F, Bissery MC, Bisagni E. Synthesis and antitumor activity of 1-[[(dialkylamino)alkyl]amino]-4-methyl-5H-pyrido[4,3-b]benzo[e]- and -benzo[g])indoles. A new class of antineoplastic agents. J Med Chem 1990;33:1519–28.
32. Vinogradov S, Roig V, Sergueeva Z, Nguyen CH, Arimondo P, Thuong NT, et al. Synthesis and binding properties of oligo-2′-deoxyribonucleotides conjugated with triple-helix-specific interca-

lators: benzo[e] and benzo[g] pyridoindoles. Bioconjug Chem 2003;14:120–35.
33. Riou JF, Fosse P, Nguyen CH, Larsen AK, Bissery MC, Grondard L, et al. Intoplicine (RP 60475) and its derivatives, a new class of antitumor agents inhibiting both topoisomerase I and II activities. Cancer Res 1993;53:5987–93.
34. Prudent R, Lopez-Ramos M, Moucadel V, Barette C, Grierson D, Mouawad L, et al. Salicylaldehyde derivatives as new protein kinase CK2 inhibitors. Biochim Biophys Acta 2008;1780:1412–20.
35. Kuo PL, Hsu YL, Chang CH, Lin CC. The mechanism of ellipticine-induced apoptosis and cell cycle arrest in human breast MCF-7 cancer cells. Cancer Lett 2005;223:293–301.
36. Yde CW, Ermakova I, Issinger OG, Niefind K. Inclining the purine base binding plane in protein kinase CK2 by exchanging the flanking side-chains generates a preference for ATP as a cosubstrate. J Mol Biol 2005;347:399–414.
37. Prudent R, Cochet C. New protein kinase CK2 inhibitors: jumping out of the catalytic box. Chem Biol 2009;16:112–20.
38. Prudent R, Moucadel V, Laudet B, Barette C, Lafanechère L, Hasenknopf B, et al. Identification of polyoxometalates as nanomolar noncompetitive inhibitors of protein kinase CK2. Chem Biol 2008;15: 683–92.
39. Meggio F, Pinna LA. One-thousand-and-one substrates of protein kinase CK2?FASEB J 2003;17:349–68.
40. Ruzzene M, Pinna LA. Addiction to protein kinase CK2: A common denominator of diverse cancer cells?Biochim Biophys Acta 2009;1804:499–504.
41. Cibull TL, Jones TD, Li L, Eble JN, Ann Baldridge L, Malott SR, et al. Overexpression of Pim-1 during progression of prostatic adenocarcinoma. J Clin Pathol 2006;59:285–8.
42. Sanjo H, Kawai T, Akira S. DRAKs, novel serine/threonine kinases related to death-associated protein kinase that trigger apoptosis. J Biol Chem 1998;273:29066–71.
43. Frantz S. Drug discovery: playing dirty. Nature 2005;437:942–3.
44. Sawyers CL. Opportunities and challenges in the development of kinase inhibitor therapy for cancer. Genes Dev 2003;17:2998–3010.